

Dénes Szilágyi

## Determination of Ultralight Helicopter Test Loads

*In recent times, more and more development activities have been taking place in our country, mainly on own resources. Some promising designs, such as the HC02.2 helicopter, are slowly reaching the milestone of type certification. This article deals with the design considerations for the related strength tests through a particular example.*

**Keywords:** *helicopter, structural loads, type certification, load cases, aerodynamic forces, load test*

### 1. Introduction

In recent times, more and more development activities have been taking place in our country, mainly on their own resources. Some of these are incipient, but others have been going on for a decade and a half and have a good industrial background. One such development is the 2-seater ultralight (UL) helicopter HC02.2 developed by Hungaro-Copter Ltd. The solutions used on this machine were developed through the construction of single-man technological demonstrators and decades of experimentation, gaining very valuable experience over time. The result of this process are some very innovative solutions, such as the fully Hungarian designed and manufactured rotor blade using the results of BERP<sup>1</sup> electric emergency propulsion, etc. In 2022, the manufacturer was granted experimental certification by the Hungarian authorities, which only allows the production of 7 units. Interest in the type is growing, thanks to the good performance at the shows. In order to meet the growing demand and the possibility of further development, the design process has now reached the stage of type-approval tests. The basis for the type certification is the (last) revision of the LTF – ULH<sup>2</sup> requirement issued by the DULV<sup>3</sup> in 2019. The DULV also performs regulatory tasks for aircraft with a maximum take-off weight of 600 kg and up to 2 seats, and their certificates are accepted by the LBA<sup>4</sup> and the Hungarian authority. Part of the certification process is to determine the loads for each structural component for the load cases specified in the regulations and to design the load (fatigue for dynamic components) tests based on these loads. This is important, not only

<sup>1</sup> BERP: British Experimental Rotor Programme. Modify helicopter rotor blades to increase the available lift and flight speed.

<sup>2</sup> LTF – ULH: Lufttüchtigkeitsforderungen für Ultraleichtflugschrauber – Airworthiness Requirements for Ultralight Helicopters.

<sup>3</sup> DULV: Deutscher Ultraleichtflugverband – German Ultralight Flying Association.

<sup>4</sup> Luftfahrt Bundesamt – German Federal Office of Civil Aviation.

to verify the strength design of the structural elements, but also because many components do not have strength design due to the completely rational copying of similar structures, and finally the interaction of the loads of the individual elements must be investigated. A good example of this is the case of the tailboom, which is subject to its own aerodynamic drag from loads generated by the horizontal and vertical stabilisers and the tail rotor. Considering the fundamentally carbon fibre construction and the fact that the relevant analysis [1, p. 11] shows that the load factor achievable by the rotor transiently is less than 2, and that mass forces can be neglected in the cases I have examined (of course, for example, for a seat load, landing gear loads, etc., mass forces are very relevant, which are basically due to loads from the ground).

## 2. Determining the loads on selected structural elements

As stated in the introduction, the design loads are given in the design specification and will be detailed for the structural element under consideration. The necessary safety factors are taken into account in point 3. The loads on the tailboom are the followings:

1. Loads coming from the tail rotor (TR) as:
  - Reaction torque of TR drive;
  - Bending moment of the Thrust of the TR;
  - Gyroscopic torque of the TR.
2. Loads coming from the stabiliser and fin as:
  - Aerodynamic drag;
  - Lift.

### 2.1. Reference load on the horizontal stabiliser

The aim of this simplified calculation is to calculate the aerodynamic loads of the stabiliser at  $V_{NE}$  with a 10 m/s wind gust from above (LTF-ULH.341 and 413). Rationale: The stabiliser in case of high speeds generates downward air force by default, for which the negative angle of attack increasing effect of the wind gust is realised.

#### 2.1.1. Determination of the aerodynamic load on the stabiliser

For the determination of the aerodynamic forces on the stabiliser (VV), the aerodynamic factors and its angle attack must be determined. For this purpose, the angle of attack of the rotor-plane has to be determined, what depends on the forces, including forces of the stabiliser (Figure 1). A simplifying assumption is that the resultant rotor thrust (TR) is balanced by the drag (D) of the fuselage and control surfaces ( $D_{FV}$  and  $D_{VV}$ ), the weight of the machine (W) and the downforce of the stabiliser ( $L_{VV}$ ). The drag of the fin ( $D_{FV}$ ) is negligibly dependent on the fuselage pitch angle (interpreted here as the slip angle). The calculation is iterative in nature as the pitch angle of the stabiliser ( $\alpha_{VV}$ ) must be estimated to give values of L and D, which I calculate to determine the pitch angle, which affects the values of L and D of the VV.

Table 1.  
Necessary data for computation [13]

|                           |                             |
|---------------------------|-----------------------------|
| $V_{NE}$ :                | <b>120 KTAS = 61.8 m/s</b>  |
| $\rho$ (ISA/SL):          | 1.225 kg/m <sup>3</sup>     |
| Dynamic pressure q:       | 2336.76 Pa                  |
| Chord of stabiliser c:    | 0.196 m                     |
| Area of stabiliser A:     | 0.21 m <sup>2</sup>         |
| Wet area of stabiliser A' | 0.22 m <sup>2</sup>         |
| Re:                       | 8.19E+05                    |
| Kinematic viscosity n:    | 0.0000148 m <sup>2</sup> /s |
| Rotor diameter D:         | 7 m                         |
| Rotor RPM:                | 577.0 1/min                 |
| Rotor $\omega_R$ :        | 60.423 1/s                  |
| Advance ratio $\mu$ :     | 0.29                        |

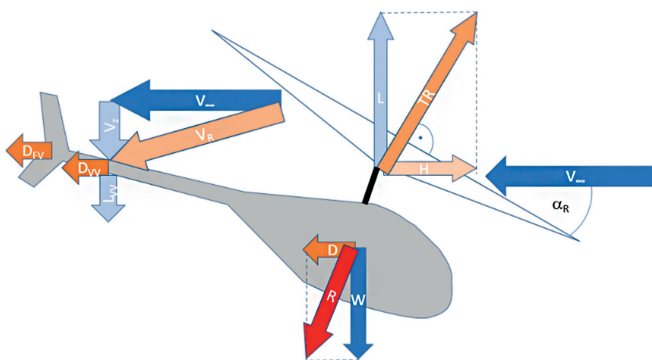


Figure 1.

Forces on the helicopter [the author]

A further assumption is that the blade tip plane is perpendicular to the rotor axis. The function of fuselage drag is based on the results of the CFD simulation of the fuselage, what was supplied by the manufacturer as from which the results of simulation titled "FC7-G üreges" have

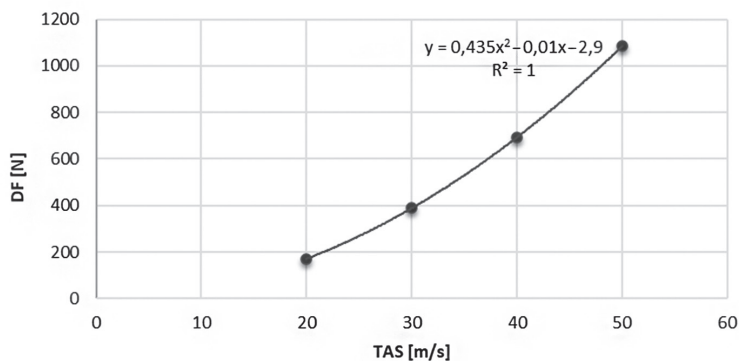


Figure 2.

Fuselage drag  $D_f$  (TAS) [the author]

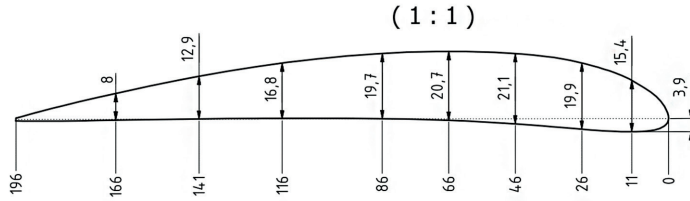


Figure 3.  
The profile of stabiliser (VV) [2]

been used. The drag of the fuselage ( $D_F$ ) as a function of TAS is shown on Figure 2. At the  $V_{NE}$  we can get a  $D_F = 1656$  N. For the calculation, I considered MTOM when the weight of the helicopter is  $W: 5886.32$  N. Calculated with  $D_F$  above and  $W$  only, the R-W angle is  $15.71^\circ$ . The installation angle of the rotor shaft is  $3.00^\circ$  (forward) and the installation angle of the VV to the tailboom is  $8.00^\circ$  (upward). By this way, the angle of attack of the VV decreases with the angle of installation of the rotor shaft and the VV, so the  $\alpha_{VV}: 4.71^\circ$ .

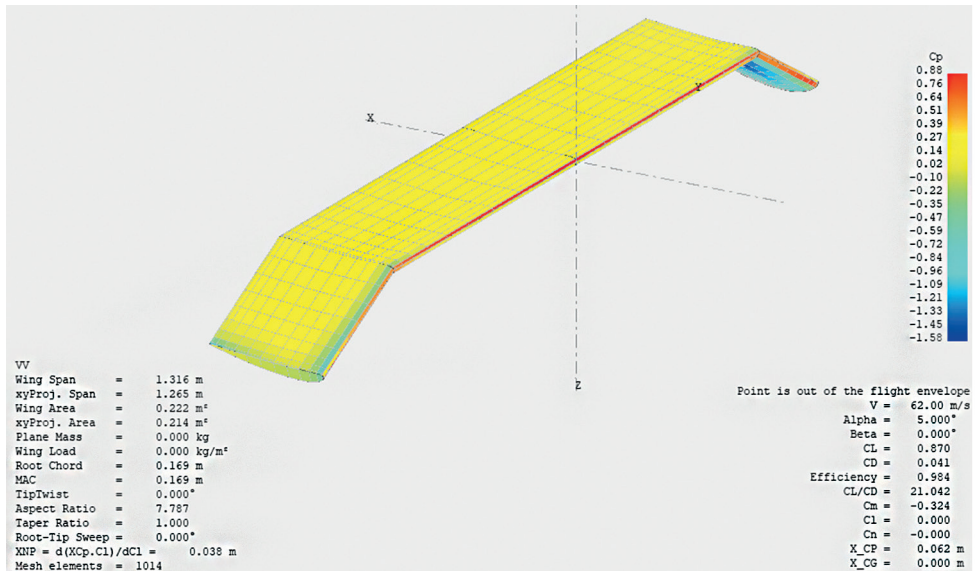


Figure 4.  
The 3D model of VV with the pressure distribution at  $\alpha_w = 0^\circ$  [the author]

On the base of these results, the aerodynamic forces of the stabiliser can be calculated. I created the VV Profile (Figure 3) properties and the whole VV behaviour with the help of XFLR5 application. The profile properties and VV parameters are shown in Figure 3, 4, and 5. As we can see on Figure 4,  $C_L = 0.87$  and  $C_D = 0.041$ . Knowing the other parameters,  $L_{VV} = 451.32$  N and  $D_{VV} = 21.27$  N. We need the Drag of the fin ( $F_V$ ) also. On the basis of XFLR5 simulation (Figure 5),  $C_D = 0.06$ . Knowing the other parameters, the  $D_{FV} = 33.23$  N.

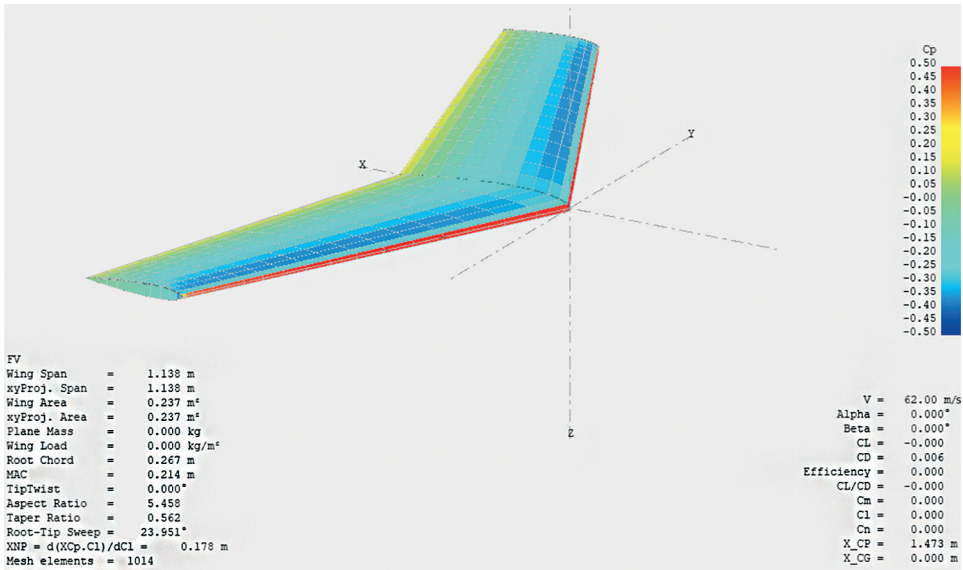


Figure 5. The 3D model of FV with the pressure distribution at  $\alpha_{VV} = 0^\circ$  [the author]

With these additional forces, the equilibrium of the helicopter was recalculated. The new drag value is balanced by the H force, so  $H = D_F + D_{VV} + D_{FV} = 1710.56 \text{ N}$  and the new necessary lift value is  $L = W + L_{VV} = 6337.65 \text{ N}$ .

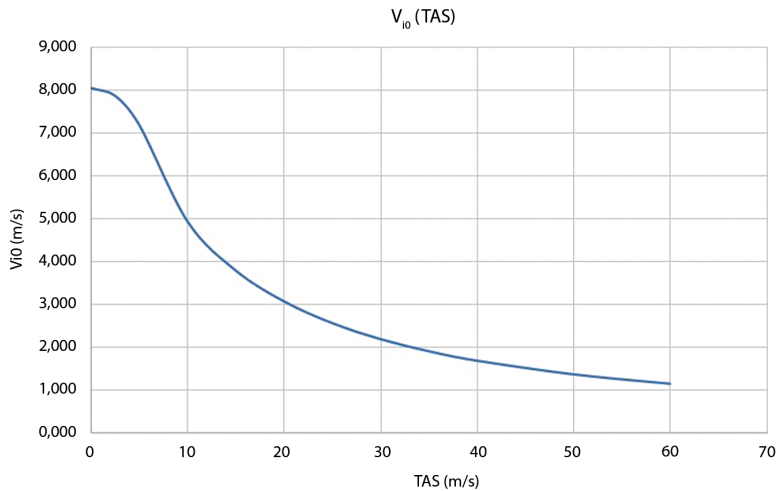


Figure 6. The average induced velocity  $v_{10}$  (TAS) [the author]

In this case, the angle of  $T_R$  with the vertical, which is equal to the value of  $\alpha_R$ , is  $15.10^\circ$ . In the verification image, the difference between the R–W angle and  $\alpha_R$  is  $\Delta\alpha_R = 0.61^\circ$ . This is a negligible difference, not worth iterating again. For the correct angle of attack of the VV, we need the induced velocity and a downstream velocity of 10 m/s of course. The [1, p. 9] serves us with the average induced speed as a function of TAS<sup>5</sup> (Figure 6), so we can get the actual  $v_{i0}$  value of 1.036 m/s. The flow of VV is given by the vector product of TAS and the 10 m/s downstream and  $v_{i0}$  vertical induced velocity.

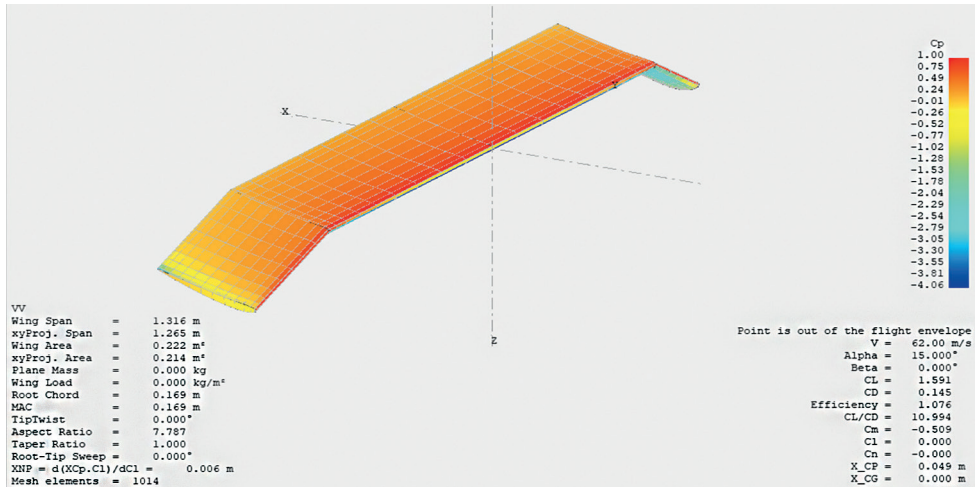


Figure 7.  
The 3D model of VV with the pressure distribution at  $\alpha_{VV} = 15^\circ$  [the author]

On this base, we can get the flow components. The vertical component  $V_z = 11.0$  m/s, the horizontal component  $V_\infty = 61.8$  m/s, the magnitude of the resulting flow  $V_R = 62.7$  m/s, the resultant angle of attack of the VV is  $f_{VV}$  of  $10.13^\circ$ . For steady horizontal flight, the  $\alpha_{VV}$  is determined (without the gust) in:  $4.71^\circ$ . By these two values, the resulting angle of attack is  $\alpha_{vvr} = \phi_{VV} + \alpha_{VV} = 14.84^\circ$ . Using XFLR5 again at this angle of attack, the  $C_L$  value is 1.591 and the  $C_D$  value is 0.145 (Figure 7). With the coefficients above knowing other parameters, the downforce on the VV at MTOM / 120 KTAS and 10 m/s downstream is  $L = 825.35$  N and  $D = 75.22$  N.

## 2.2. The reference load of fin (FV)

The aim of this simplified calculation is to calculate the aerodynamic loads of the fin as prescribed by the LTF-ULH.351. By this way, we have to suppose a  $90^\circ$  drift at the 60% of the  $V_{NE}$  and a  $15^\circ$  drift at the  $V_{NE}$ . Both cases shall be calculated, and then the larger value can be used for strength test. The fin is a swept back asymmetric construction, see Figure 8.

<sup>5</sup> TAS: True Air Speed.

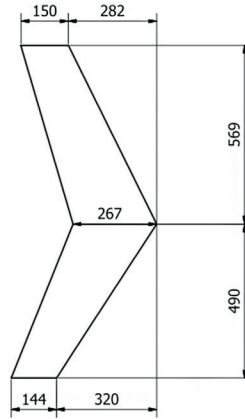


Figure 8.  
Fin [11]

### 2.2.1. Determination of the aerodynamic load on the fin

The LTF-ULH.351 a) assumes a slip angle of 15 degrees at  $V_{NE}$ . The slip angle = angle of attack of the fin supposed for the calculation (effect of MR downwash is not considered). The  $C_L$  of the profile from [3, p. 4] is about 1.33. Considering the shape using XFLR 5, we can get a  $C_L$  of 1.074,  $C_D$  of 0.082, and  $\epsilon = 7.9\%$  (Figure 9). Further simplifications:

- the chord and the tailboom are parallel (there is a difference of 3 degrees in the reality);
- the drag is 7.9% of the lift and pulls the tailboom;
- the induced velocity of the tail rotor is less than 1 m/s, so its effect has not been considered on the zone of fin affected by the downwash of the TR;
- the asymmetry of the fin (top part area is  $0.118 \text{ m}^2$  and the bottom one is  $0.1 \text{ m}^2$ ) is also not considered as a source of twisting moment.

The results of calculation are  $L_{FV} = 533.4623618 \text{ N}$  and  $D_{FV} = 42.02 \text{ N}$ .

Table 2.  
Necessary data for computation [13]

|                                |                             |
|--------------------------------|-----------------------------|
| $V_{NE}$ :                     | <b>120 KTAS = 61.8 m/s</b>  |
| $\rho$ (ISA/SL):               | 1.225 kg/m <sup>3</sup>     |
| Dynamic pressure q:            | 2336.76 Pa                  |
| Root chord c:                  | 0.267 m                     |
| MAC of fin:                    | 0.214 m                     |
| Area of stabiliser A:          | 0.2193 m <sup>2</sup>       |
| Wet area of stabiliser A'      | 0.234 m <sup>2</sup>        |
| Leading edge sweep back angle: | 23.951°                     |
| Re:                            | 8.94E+05                    |
| Kinematic viscosity n:         | 0.0000148 m <sup>2</sup> /s |
| Profile of the fin:            | NACA 0012                   |



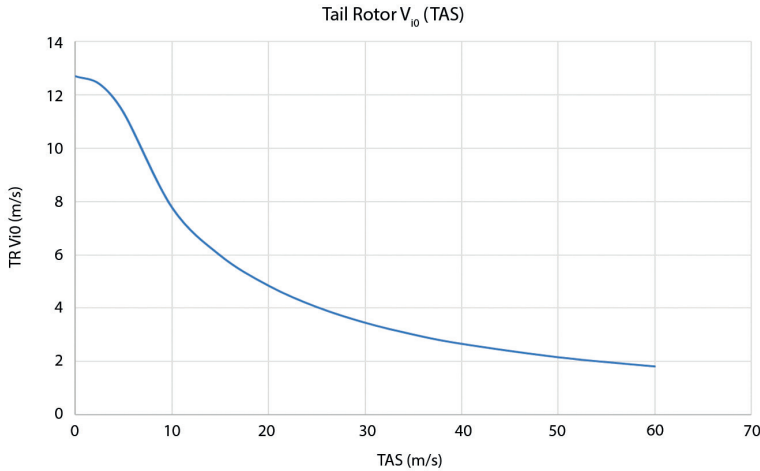


Figure 10.  
*v<sub>i0</sub> of the TR [the author]*

Knowing all other parameters, the magnitude of the drag force on the fin is:  $D_{FV} = 383.72 \text{ N}$ .

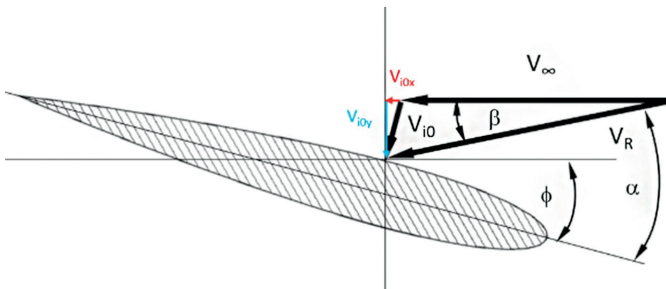


Figure 11.  
*Effect of v<sub>i0</sub> on fin [the author]*

By this way, the significant load is in case of the 15 degrees slip. The strength test of the fin, therefore, shall be designed for this value.

### 2.3. Loads generated by the tail rotor (TR)

The TR generates reaction torque on its drive, what is in parallel appears as a constant bending moment along the tailboom, the thrust of the TR what bends the tailboom also, and finally in case of any rotating motion, the inertia of the TR can generate a gyroscopic torque of the TR.

### 2.3.1. Determination of the maximum achievable TR thrust value

As a first step, the calculation of the power necessary to the TR – supplied by the tail-gearbox (TGB) – shall be determined. Unfortunately, in the lack of this TGB-out power, the whole transmission shall be analysed. The effective power of the Rotax 915i engine in case of take-off power setting is:  $P_{\text{eff}} = 104 \text{ kW}$  at 5800 RPM. As  $\omega = 2 \pi n$ , the moment of the engine is:

$$M = \frac{P_{\text{eff}}}{\omega} = 171.229 \text{ Nm} \quad (1)$$

In case of maximum cruise power (MCP) setting, we have  $P_{\text{eff}} = 99 \text{ kW}$  at 5500 RPM what gives  $M_{\text{MCP}} = 171.887 \text{ Nm}$  moment. The power values above shall be considered as available power on the output shaft of Rotax 915i gearbox. The gear ratio of this gearbox is  $i = 2.54545$ . On the base of the moment results above, the take-off power considered as  $P_{\text{out}}$  for further calculation. With the gear ratio above, the output angular velocity of the gearbox is  $\omega_{\text{out}} = 238.612 \text{ 1/s}$  ( $n_{\text{out}} = 2278.575 \text{ RPM}$ ). With this value,  $M_{\text{out}} = 435.854 \text{ Nm}$ . The power is transmitted from the engine to the transmission shaft via vee-belts, as can be seen in Figure 12. Ratio of this vee-belt transmission is:  $i_{\text{DB}} = 0.67347$ . The effectiveness of this vee-belt transmission is (declaration of the manufacturers):  $\eta_{\text{VBT}} = 0.97$ . By this way, the input power on transmission shaft is:  $P_{\text{in}} = P_{\text{out}} \eta_{\text{VBT}} = 100.88 \text{ kW}$ . Furtherly, the RPM of the transmission shaft is:  $n_{\text{in}} = \frac{n_{\text{out}}}{i_{\text{DB}}} = 3383.336 \text{ RPM}$ .

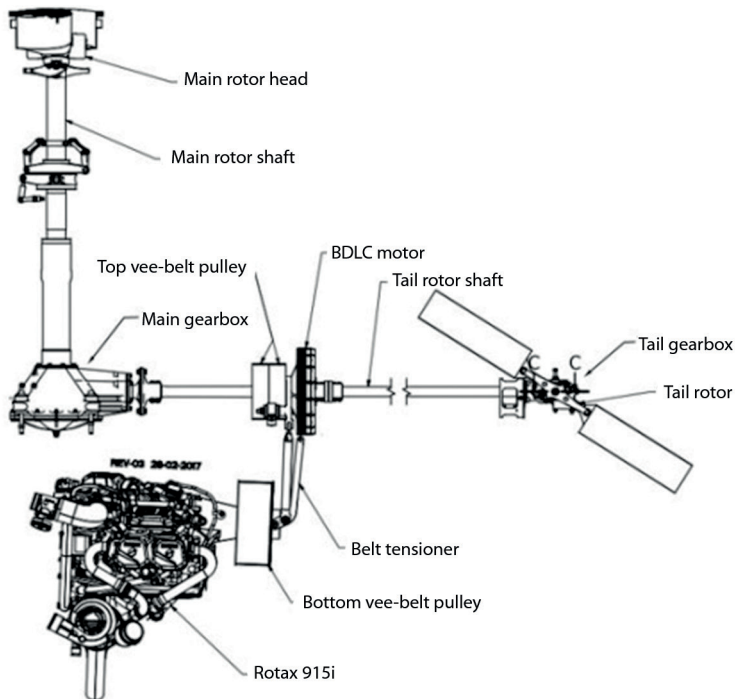


Figure 12.  
HC-02.2 Transmission system [10]

The following values are given by the manufacturer, and coincide with the literature.

The maximum input power of tail gearbox (TGB) was measured by the control of the emergency electric drive when the MGB was disconnected:  $P_{TGBin} = 13$  kW. The input power of main gearbox (MGB):  $P_{MGBin} = P_{in} - P_{TGBin} = 87.88$  kW with  $\omega_{MGBin} = 354.302$  1/s (without details). Knowing the  $\omega_{MGBin}$ , the input torque of MGB is:  $M_{MGBin} = 248.037$  Nm. Gear ratio of MGB:  $i_{MGB} = 5.85714$ . The power loss of the MGB is (declaration of the manufacturer): 2%, so  $\eta_{MGB} = 0.98$ . Using this efficiency, the output power of MGB to the main rotor head (MRH) is:

$$P_{MR} = \eta_{MGB} P_{MGBin} = 86.122 \text{ kW} \quad (2)$$

As we know the gear ratio and  $\omega_R = 60.491$  1/s, the torque of MR is  $M_{MR} = \frac{P_{MR}}{\omega_R} = 1423.731$  Nm. The input RPM of the MGB and TGB is the same. Therefore, the input torque maximum of TGB is:

$$M_{TGBin} = \frac{P_{TGBin}}{\omega_{MGBin}} = 36.692 \text{ Nm} \quad (3)$$

The gear ratio of the TGB is:  $i_{TGB} = 0.9545$ . The angular velocity of tail rotor (TR):

$$\omega_{TR} = \frac{\omega_{MGBin}}{i_{TGB}} = 371.191 \text{ 1/s} \quad (4)$$

The power loss of the TGB is (declaration of the manufacturer) also 2% so  $\eta_{TGB} = 0.98$  and the output power of the TGB is:

$$P_{TGBout} = \eta_{TGB} P_{TGBin} = 12.74 \text{ kW} \quad (5)$$

On this base, the torque n of tail rotor is:

$$M_{TR} = \frac{P_{TGBout}}{\omega_{TR}} = 34.322 \text{ Nm and } n_{TR} = 3544.616 \text{ RPM} \quad (6)$$

The other components of necessary power have same percentages as below, and were considered with the 104 kW available power of Rotax 915i for control purposes. On the base of [4, p. 46], the following engine power output percentages are generally in case of a tail rotor helicopter:

- for the main rotor drive cca. 75–80%
- for the tail rotor drive cca. 8%
- artificial cooling of the piston engine needs cca. 5%
- the friction loss of the transmission needs cca. 7%
- drive of auxiliary equipment needs cca. 1–2%

Based on the values above, the total power loss should be 16–17%, so the power available (real) for the main rotor is:

$$P_{MRreal} = P_{eff} 0.83 = 86.32 \text{ kW} \quad (7)$$

so the suppose of  $P_{MR} = 86.122$  kW is realistic, that's why the further calculation is based on this value. In hover, the necessary thrust of TR for balancing (vertical climb and steep turn should be simulated) can be calculated, knowing the torque of MR and the distance ( $L_{TR}$ ) of MR axis and TR axis in the plane what is perpendicular to the MR axis.

$$L_{TR} = 3.9925 \text{ m, so the thrust of TR is: } T_{TR0} = \frac{M_{MR}}{L_{TR}} = 356.601 \text{ N} \quad (8)$$

The thrust of tail rotor should be estimated on the base of statistics with the following relationship [4, p. 120]:

$$T_{TRstat} = 30 P_{TGBout} \text{ (in kW)} = 382.2 \text{ N (instead of kW)} \quad (9)$$

Therefore, the TR could ensure the necessary balancing thrust if it took such power. Nevertheless, by this way, there is only 24 N as reserve control thrust, what is not so much. Since the rate of necessary powers is:

$$\frac{P_{TGBout}}{P_{eff}} = 12.25\% \quad (10)$$

Namely, this value is 1.5 times higher than the 8% above; this value must contain the necessary thrust for directional control also. Remark: In case of Mi-8 helicopter, the TR takes 530 HP of the available 3000 HP what is 17.7%, in case of fully deflected pedals without any yawing (yaw turn decreases the necessary power). These results are not so coincident.

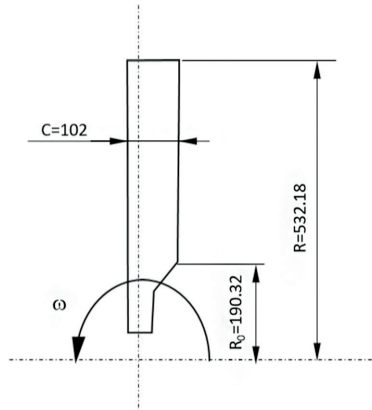


Figure 13.  
Tail rotor geometry [12]

For further clarification, the thrust (and its distribution along the blades\*) has been calculated with the combined Blade-element – Momentum Theory. The necessary data (Figure 13) for calculation:

- Data of TR:
- R = 532.18 mm
- C = 102 mm
- D = 1.06436 m
- R<sub>0</sub> = 190.32 mm
- δ = 0.119
- ρ = 1.225 kg/m<sup>3</sup>



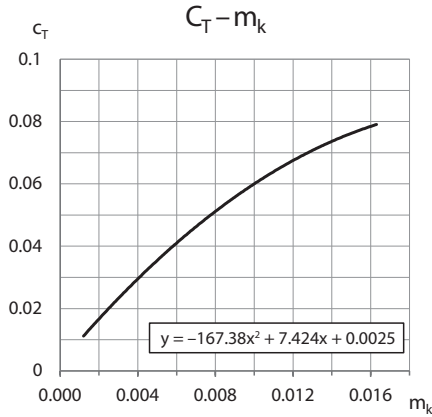


Figure 15.  
 $c_T - m_k$  curve source [7, p. 17]

The Manufacturer shared the range of pitch is  $\phi$  from  $-9^\circ$  (RH pedal max) to  $+15^\circ$  (LH pedal max) at the 0.75R. As we can see on the base of  $\phi_{R075}$ , there is  $4.7^\circ$  control reserve (LH pedal) in case of hovering until the opposite direction there is a much higher control range ( $19.3^\circ$ ) estimated. As a first step, we can calculate the  $m_k$  torque factor on the base of the maximum  $M_{TR}$  calculated formerly:

$$m_k = \frac{2M_{TR}}{\rho(\omega_{TR})^2 A_{TRR}} = 0.0039721 \quad (16)$$

For this  $m_{k1}$  value, we can find the appropriate  $c_{T1}$  value for 1 m diameter experimental rotor of [7, p. 17, figure 1.8]. Look at Figure 15 with the equation of trend line. With the trend equation, we can get the  $c_T = 0.0029348$ . With this  $c_T$  value, we can calculate the maximum achievable thrust of the TR with the following formula:

$$T_{TRmax1} = c_{T1} \rho/2 (R\omega)^2 A_s = 517.42 \text{ N} \quad (17)$$

Knowing the  $T_{TR0}$  (necessary thrust for MR balancing in case of steady hover), the  $c_{T2}$  can be calculated:

$$c_{T0} = \left( \frac{2 T_{TR0}}{\rho(R\omega_{TR})^2 A_s} \right) = 0.0202 \quad (18)$$

for which the  $m_k$  value from Figure 15  $m_{k0} = 0.002532$ . With this value, the  $M_{TR0} = 23.75 \text{ Nm}$  and the  $P_{TR0} = 8.03 \text{ kW}$ . In case of hover, a rough approximation of the thrust is proportional to the pitch if the RPM remains unchanged [8, p. 191] (Figure 16).

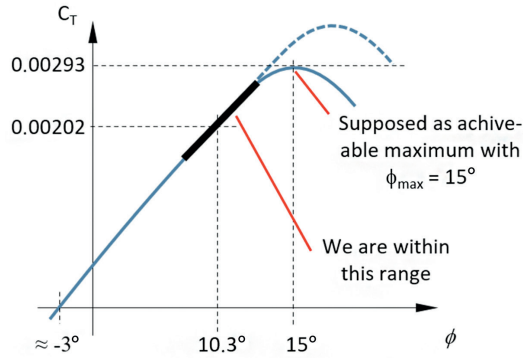


Figure 16.  
Generic  $c_T(\phi)$  [the author]

Just for checking the calculation, the maximum thrust was also calculated on the base of the rate of  $c_T(\phi)$  values. From Figure 15, the  $\phi$  for  $c_T = 0$  can be assumed as  $-3^\circ$  averagely, if by the value of  $\phi_{R075} = 10.3^\circ$  when the  $T_{TR0} = 356.601$  N. By this way, the tangent of the linear section of the  $c_T(\phi)$  curve:

$$\frac{dc_T}{d\phi} = 0.0015208 \quad (19)$$

Using this tangent value, we can calculate the  $c_T$  of  $\phi_{R075} = 18^\circ$  which is  $c_{T2} = 0.02737$ . By this way, we can re-calculate the  $T_{TR}$  using the rate of  $c_T$  values, what is:

$$\frac{c_{T2}}{c_{T0}} = 1.35 \quad (20)$$

By this way, the  $T_{TR}$  value is:  $T_{TR2} = 482.61$  N. Just for checking purpose, the thrust factor was determined also with the following formula used for propellers:

$$T_{TR2} = c_T \rho n'^2 D^4 \quad (21)$$

where  $n'$  is the revolution per second ( $n_{sec}$  below). As this expression is used for propellers basically, such  $c_T$  values are not directly comparable to the above ones but give a good basis.

$$n_{sec} = \frac{\omega_{TR}}{2\pi} = 59.077 \text{ 1/s and with this value the } c_{Tmax} = \left( \frac{2T_{TR2}}{\rho n_{sec}^2 D^4} \right) = 0.088 \quad (22)$$

This value looks like a usual value for  $TAS = 0$  (hovering) on the base of curves in the [9, p. 47] (Note: the  $c_T$  values there must be multiplied by 2 due to the use of  $\rho/2$  there, instead of  $\rho$  here and the present  $\sigma = 0.119$  which is higher than 0.1 there). On the base of this, we can accept the  $T_{TR2}$  value above as a realistic one (generated with maximum pedal movement in the direction of MR rotation during hovering). Nevertheless, on the base of Figure 15, we can see the maximum experimental  $c_T$  values were close to 0.08. When the maximum power required by the TGB was measured, the Manufacturer used the maximum value of  $\phi = 15^\circ$ .

It can be seen, there should be more reserves in the TR, therefore, the  $T_{TR1}$  values are suggested to be used for certification purpose. Additionally, the 1.5 factor of LTF-ULH 351 also shall be considered. By this way during the load test, the suggested force below shall be applied in the axis of TR shaft pushing it to the right side of the helicopter (counter-clockwise):  $T_{TR} = 776.13 \text{ N}$

The reaction torque of the TR can be calculated on the base of the  $P_{TGBout} = 12.74 \text{ kW}$ , given it is a realistic value necessary to the maximum thrust above.

### 2.3.2. Determination of the TR reaction torque value

On the base of LTF-ULH.361, the torque of a four stroke 4-cylinder piston engine shall be considered with a multiplication factor of 2 due to the torque fluctuation of the engine. The case in LTF-ULH.337 does not result higher torque on the TGB than calculated in (5) above, because the maximum available power is used in both cases. In other words, the TGB cannot consume more power than 13 kW. By this way, the reaction torque of the TR is:

$$M_{TR} = \left( \frac{2 P_{TGBout}}{\omega_{TR}} \right) = 68.644 \text{ Nm} \quad (23)$$

and shall be considered with opposite direction of TR rotation.

### 2.3.3. Determination of the TR gyroscopic moment value

We are examining a rotor where the flapping motion is allowed, and in case of a flapping deflection, the pitch change rods modify the  $\phi$  to counteract that deflection. This is in case of a deflection caused by gyroscopic moment. As the experiment with plasticine (Figure 17) shows, the tail rotor blades do not reach the end of range of flapping motion even with the most intense yawing motion (video also available), so gyroscopic torque cannot be generated and does not load the tailboom.



Figure 17.  
Effect of flapping compensation [13]

### 3. Planning of the load tests

For the loads defined in Chapter 2, LTF – ULH also provides various load, handling, operational, and safety factors. The main problem is the rather general wording of the requirements, which causes problems for the user. There are difficulties in interpreting which loads are sufficient to be applied individually, and which must be applied simultaneously. The case of the tailboom is also a good example. It also seems impossible, given the flight experience and the power demand, for the helicopter to perform 15 degrees slip at  $V_{NE}$  under its own power. However, no lateral gust should be prescribed, only a vertical gust to verify the VV. However, if we assume the feasibility of this slip, we find that the thrust of the TR and the lift on the FV are in opposite directions and balance each other out to a significant degree. Hence, there is hardly any torque on the tailboom, while the TR thrust and the FV forces are at their maximum, so they should be tested separately. If there were also a lateral gust, then the TR thrust and the FV lift would sum, subjecting the tailboom to significantly more bending. In any case, the FV would have to be dismantled to apply the distributed load. The points of attack of the forces and torque are clearly determined, therefore, after the calculation of the load a strength test of the tailboom can be easily carried out.

#### 3.1. Determination of data necessary for strength test of horizontal stabiliser

For determination of the load to be applied, we must assume a square load distribution (as per ULH.427, which results higher than real bending moment values). The half of the stabiliser bears half of the load that is  $L/2$ : 619.01 N, considering the 1.25 and 1.5 factors. The half of the span is  $S/2 = 609.00$  mm. With these two values, the specific lift is:  $L/S = 1.02$  N/mm. For the simulation (strength test) of the  $L_{VV}$ , a mass distribution can be calculated for a practical number of segments (Figure 18) along the span of stabiliser. From this, the force acting on each segment and the required mass for its simulation can be calculated. The twisting moment of the profile of VV also must be considered. The next task is to create a twist by moving the point of contact. The mass forces are omitted because of the light construction and the opposite effect to the  $L_{VV}$ . In the simulation with XFLR5, the centre of pressure of the VV profile is 10.68% from the inlet. The torque factor of the profile:  $c_m = -0.509$ . With this  $c_m$  the total torque on half VV is:

$$M = c_m q c A/2 = -25.88 \text{ Nm} \quad (24)$$

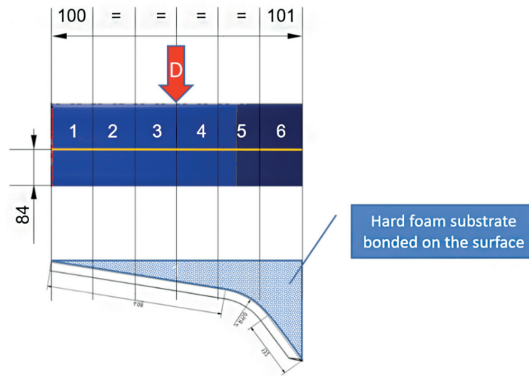


Figure 18.  
Load distribution along the half stabiliser (VV) [the author]

For simulating this effect, the load imitating mass should be placed further back than Aerodynamic Centre (hereafter AC) of profile. The distance from AC can be determined from the expression  $M = x L/2$  where  $x = -4.2$  mm (negative means behind the AC). Since VV is rectangular in projection, this is a constant value along the span. By this amount, the centre of mass of the loads must be placed behind AC. Knowing the necessary distance from the leading edge is more practical. It is 62.74 mm and indicated by the orange line on the top view of Figure 18. The stabiliser is anhedral with the angle of  $9^\circ$ . This arrangement results in a more unfavourable lift distribution along the stabiliser and reduces the resulting moment arm of the lift. The projection of half of the stabiliser is thus 601.5 mm. Compared to the calculation carried out assuming a horizontal arrangement, this results in lower loads (lift and its bending moment), which I have not considered, thus also deviating towards safety. By using the foam interlayer, as shown in Figure 18, the loads on each strip can be easily applied. Due to the small value of the drag, it is not necessary to apply it as a distributed load along the entire span. The point of attack of D shall be applied at 301 mm from the root at half the span of the VV rearwards in its plane due to the assumption of an angular distribution (it is recommended to use at least 100 mm wide strap when applying the load). Using the specific lift above and the length of segments for the imitation of the  $L_{VV}$ , the load to be loaded in zones 1–5 is 12.395 kg and in zone 6 is 13.73 kg.

### 3.2. Determination of data necessary for strength test of fin

Determination of the load to be applied assuming a square (as per ULH.427) load distribution. Due to the asymmetry of the fin, the whole fin must be loaded. I consider the atmospheric loads to be proportional to the surface along the span, so the effect of the pressure equalisation at the tip has not been considered. This gives the resulting point of attack moved further away from the root, resulting in a higher bending moment. The surface of the fin should be divided into 100 mm wide strips. The uniform surface load is  $0.002432569 \text{ N/mm}^2$  on which base the necessary mass values can be calculated for each strip, as shown in Table 3 below.

Table 3.  
Loads for strength test of the fin [the author]

| Location ID | Mid of strip [mm] | Mean chord MC [mm] | Area of strip [mm <sup>2</sup> ] | The Lift on the strip L' [N] | Factor (§ 351) | Factor (§ 619) | Factor (§ 303)                         | Imitation mass [kg] | Point of attack from the LE [mm] |
|-------------|-------------------|--------------------|----------------------------------|------------------------------|----------------|----------------|--|---------------------|----------------------------------|
| F6          | 535.00            | 156.99             | 10832.39367                      | 51.77                        | 1.5            | 1.25           | 1.5                                    | 14.84               | 70.65                            |
| F5          | 450.00            | 174.47             | 17446.92443                      | 83.38                        | 1.5            | 1.25           | 1.5                                    | 23.90               | 78.51                            |
| F4          | 350.00            | 195.03             | 19503.16344                      | 93.21                        | 1.5            | 1.25           | 1.5                                    | 26.72               | 87.76                            |
| F3          | 250.00            | 215.59             | 21559.40246                      | 103.04                       | 1.5            | 1.25           | 1.5                                    | 29.54               | 97.02                            |
| F2          | 150.00            | 236.16             | 23615.64148                      | 112.86                       | 1.5            | 1.25           | 1.5                                    | 32.36               | 106.27                           |
| F1          | 50.00             | 256.72             | 25671.88049                      | 122.69                       | 1.5            | 1.25           | 1.5                                    | 35.17               | 115.52                           |
| A1          | 50.00             | 254.45             | 25444.89796                      | 121.61                       | 1.5            | 1.25           | 1.5                                    | 34.86               | 114.50                           |
| A2          | 150.00            | 229.35             | 22934.69388                      | 109.61                       | 1.5            | 1.25           | 1.5                                    | 31.42               | 103.21                           |
| A3          | 250.00            | 204.24             | 20424.4898                       | 97.61                        | 1.5            | 1.25           | 1.5                                    | 27.98               | 91.91                            |
| A4          | 350.00            | 179.14             | 17914.28571                      | 85.62                        | 1.5            | 1.25           | 1.5                                    | 24.54               | 80.61                            |
| A5          | 445.00            | 155.30             | 13976.63265                      | 66.80                        | 1.5            | 1.25           | 1.5 </td <td>19.15</td> <td>69.88</td> | 19.15               | 69.88                            |

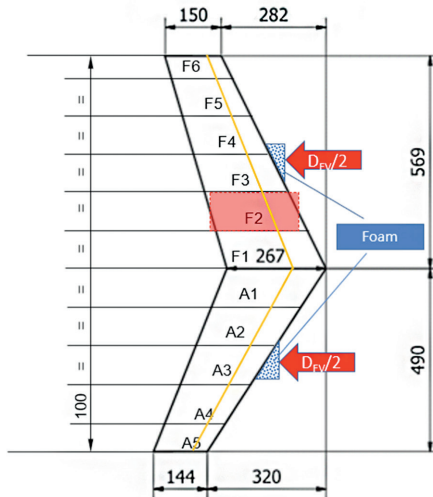


Figure 19.  
Load distribution along the fin (FV) [the author]

The  $c_m$  of the profile is a small but no zero value, [3, p. 16]  $c_m = 0.02$  and the distance of the AC from the leading edge (LE) at  $\alpha = 15^\circ$  is 22%. The twist moment for each segment can be calculated as follows:

$$M = c_m q MC A \tag{25}$$

On this base, the necessary distance from the LE to create a twist can be calculated (orange numbers in Table 3) as a sum of the moments from the tip to the root (summary column in Table 3).

$$l = MR/L' + c_m MC \quad (26)$$

Figure 19 shows the location of each strip. The orange line shows the location of the centre of gravity of the applied loads. The red rectangle shows the equivalent area of the particular strip. Due to the small value of the Drag, it is not necessary to apply it as a distributed load along the entire span. For simplifying  $D_{FV}/2 = 6 \text{ kg}$  values (the 1.5 load factor of § 351, the safety factor of 1.25 as per § 619 and 1.5 as per § 303 already considered) shall be applied at halves of spans (bottom 245 mm and top 298 mm) from the root of the FV rearwards in its plane due to the assumption of an angular distribution. It is recommended to use a 100 mm wide strap and hard foam substrate when applying the load.

### 3.3. Determination of necessary data for tailboom strength test

The details of calculations are comprised by their particular document. Only the results are stated here:

- according to LTF-ULH.341, 413, the stabiliser shall be examined for the case of  $V_{NE}$  (120 KTAS supposed) with a 10 m/s wind gust from above. In this case the Lift on the stabiliser is  $L_{SV} = 825.35 \text{ N}$ ;
- according to LTF-ULH.351, the lateral loads on the fin in case of the LTF-ULH.351 a) assumes a slip angle of 15 degrees at  $V_{NE}$  has given the higher lift value  $L_{FV} = 533.46 \text{ N}$  what shall be multiplied by the 1.5 factor of LTF-ULH.351 so this  $L_{FV} = 800.19 \text{ N}$ . As we can see, the side force on the fin is higher than the maximum thrust of the TR.

### 3.4. Summary of results

The load test of the tailboom can be executed as shown in Figure 20. In this case, we supposed the simultaneous existence of a sudden and maximum pedal deflection and a 10 m/s downstream at  $V_{NE}$ . The moment distributions on the Figure 20 are only illustrative because there are two struts even at the mounting of the horizontal stabiliser.

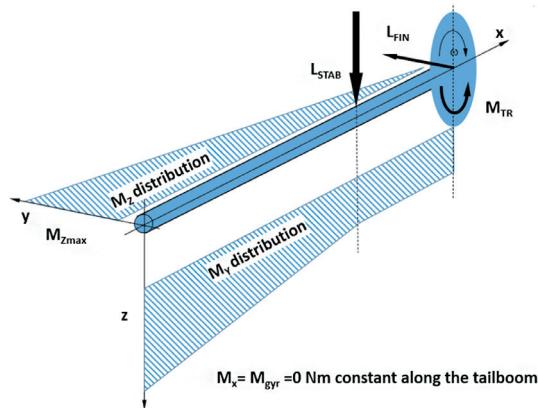


Figure 20.  
Loads on the tailboom [the author]

For the load test, the safety factor 1.5 required by LTF-ULH.303 and the factor 1.25 required by LTF-ULH.619 must be considered. The  $M_{TR}$  contains the safety factor of 2 as per ULH.337. By this way, the forces to be applied during the strength test of the tailboom are:

- a)  $L_{FIN} = 1261.025 \text{ N}$  (1.5  $\times$  1.25  $\times$  1.5 factors included)
- b)  $L_{STAB} = 1547.529 \text{ N}$  (1.25  $\times$  1.5 factors included)
- c)  $M_{TR} = 68.644 \text{ Nm}$  ( $\times$  2 factor included, concentrated on the TGB)

The loads in a) and c) points above and the loads in points b) and c) shall be applied simultaneously. All loads shall be applied at least for 3 seconds.

## 4. Conclusion

Designing load tests requires a thorough knowledge of the specifications and the aircraft structure. In addition, the design of the load tests is greatly influenced by the load cases that may occur simultaneously and the technical possibilities for simulating them simultaneously, since it is useful to test everything in situ without dismantling. In this case, the interaction of the loads on the different structural elements must also be taken into account. Therefore, it is advisable to start the load tests when the prescribed loads of all the elements to be tested have been established.

## References

- [1] D. Szilágyi, *Definition of maximum achievable  $n_z$  coefficient*. HungaroCopter Report No EX330, 2023.
- [2] Drawing No. HC02.2HS-55-10, HungaroCopter Ltd. 2023.
- [3] NACA TECHNICAL NOTE 3361.
- [4] Gy. Szelestey, *Helikopterek I*. MGF Nyiregyháza 1985.
- [5] Airfoil Tools, *Airfoil Catalogue data of NACA 2412*. Online: <http://airfoiltools.com/polar/details?polar=xf-naca1412-il-1000000>
- [6] Airfoil Tools, *Airfoil Catalogue data of NACA 2414*. Online: <http://airfoiltools.com/polar/details?polar=xf-n2414-il-1000000>
- [7] Л. С. Вильдгрубе, *Вертолеты. Расчет интегральных аэродинамических характеристик и летно-технических данных*. Москва, Машиностроение, 1977.
- [8] J. Rohács, Zs. Gausz, T. Gausz, *Aerodinamika*. BME. Online: <http://dtk.tankonyvtar.hu/xmlui/handle/123456789/3252>
- [9] P. A. Янг, *Теория и расчет геликоптера* ОБОРОНГИЗ. 1951.
- [10] Certification Programme No: DX001 HungaroCopter Ltd. pp. 16. 2023.
- [11] Drawing No. HC-02.2 VS-55-30-01-V01, HungaroCopter Ltd. 2022.
- [12] Drawing No. HC-02.2 HS-55-10-09-V01, HungaroCopter Ltd. 2023.
- [13] Declaration of the manufacturer.

---

## ***Ultrakönnyű helikopter vizsgálati terheléseinek meghatározása***

*Az utóbbi időben hazánkban egyre több fejlesztési tevékenység folyik, alapvetően saját erőből. Néhány ígéretes konstrukció, így a HC02.2 helikopter is lassan eljut a típusalkalmassági vizsgálatok mérföldkövéhez. Az ezzel kapcsolatos szilárdsági vizsgálatok tervezésének kérdéseivel foglalkozik ez a cikk egy konkrét példán keresztül.*

**Kulcsszavak:** *helikopter, szerkezeti terhelések, típusalkalmasság, terhelési esetek, aerodinamikai erők, terhelési próba*

---

Dr. Szilágyi Dénes  
egyetemi docens  
Nyíregyházi Egyetem  
Műszaki és Agrártudományi Intézet  
Közlekedéstudományi és Infotechnológiai  
Tanszék  
[szilagyι.denes@nye.hu](mailto:szilagyι.denes@nye.hu)  
[orcid.org/0000-0001-6055-0010](https://orcid.org/0000-0001-6055-0010)

---

Dénes Szilágyi, PhD  
Associate Professor  
University of Nyíregyháza  
Institute of Engineering and Agriculture  
Department of Transportation and  
Infotechnology  
[szilagyι.denes@nye.hu](mailto:szilagyι.denes@nye.hu)  
[orcid.org/0000-0001-6055-0010](https://orcid.org/0000-0001-6055-0010)

---